Annals of Biomedical Engineering
https://doi.org/10.1007/s10439-025-03696-0

BMES BIOMEDICAL ENGINEERING SOCIETY

ORIGINAL ARTICLE

Controlling Negative and Positive Power for Efficiency Enhancement and Muscle Strain Mitigation During Squatting with a Portable Knee Exoskeleton

Shuangyue Yu[1,2] · Lu Liu[1] · Sainan Zhang[2] · Antonio Di Lallo[2] · Junxi Zhu[2] · Qifei Wu[1] · Guoyu Zuo[1] · Xianlian Zhou[3] · Hao Su[2,4]

Received: 20 May 2024 / Accepted: 18 February 2025

Abstract

Purpose Workers face a notable risk of musculoskeletal injuries when performing squatting tasks. Knee exoskeletons offer a promising solution to mitigate muscle strain through squat assistance. However, existing studies on knee exoskeletons lack a comprehensive study that meets the multifaceted requirements of squatting assistance in terms of portability, efficiency, and muscle strain mitigation. Furthermore, another open research question pertains to the control strategy of squat assistance, which should be adaptable to various postures and cadences for different individuals. In particular, the effect of controlling negative power assistance during the squat-down phase is not studied.

Methods To fill these two gaps, first, we develop a simple (computationally efficient and implementable in a microcontroller) and generalizable (for different postures, cadences, and individuals) torque controller for portable knee exoskeletons that delivers both negative and positive power. Our portable knee exoskeleton can benefit users by enhancing efficiency (reducing metabolic cost, heart rate, breathing ventilation), mitigating muscle strain (reducing EMG), and reducing perceived exertion (reducing Borg 6–20 scale) during squatting. Second, we study the effect of three levels of negative power assistance during the squat-down phase.

Results This study integrates comprehensive biomechanics and physiology analyses that evaluate our exoskeleton's effectiveness using four objective and two subjective metrics with a group of able-bodied subjects ($n=7$). The exoskeleton reduced metabolic cost by 12.8%, heart rate by 13.8%, breathing ventilation by 8.9%, and reduced extensor muscle activity by 39.4–43.2%, flexor muscle activity by 18.9–20.3%, and Borg perceived exertion rate by 1.8 during squatting compare with not wearing the robot.

Conclusion Different from the musculoskeletal model predictions that suggest increasing benefit with a higher level of negative power assistance, we find that the best performances were achieved with a moderate level of negative power assistance, followed by no assistance and then high assistance.

Keywords Wearable robotics · Portable knee exoskeleton · Squatting · Negative power · Dynamic model

Associate Editor Joel Stitzel oversaw the review of this article.

✉ Guoyu Zuo
zuoguoyu@bjut.edu.cn

✉ Hao Su
hao.su@nyu.edu

[1] Faculty of Information Technology and the Beijing Key Laboratory of Computing Intelligence and Intelligent Systems, Beijing University of Technology, Beijing 100124, China

[2] Lab of Biomechatronics and Intelligent Robotics, Department of Biomedical Engineering, Tandon School of Engineering, New York University, Brooklyn, NY 11201, USA

[3] Department of Biomedical Engineering, New Jersey Institute of Technology, Newark, NJ 07102, USA

[4] Department of Mechanical and Aerospace Engineering, North Carolina State University, Raleigh, NC 27695, USA

Published online: 17 March 2025

Introduction

Workers perform repetitive squatting movements in industrial scenarios. These movements are often associated with considerable physical demand, which requires high lower-limb flexibility and strength, potentially leading to the risk of work-related musculoskeletal disorders (MSDs) [1–3]. Squatting activities impose significant loads on the lower-limb joints, leading to elevated contact stress and predisposing the tibiofemoral and patellofemoral joints to injury [4]. Exoskeleton technology promises to reduce the user's muscle effort and energy expenditure [5–8].

Wearable devices designed for squat assistance, including passive [9–11], semi-passive [12], and semi-active [13] systems, employ energy storage mechanisms such as springs and elastic straps to store and release energy. While these designs have shown efficacy in reducing muscle activities over multiple trials, they are limited to providing pre-defined assistance profiles. In contrast, active exoskeletons address this limitation by injecting power into the user and offering controllable assistance. For instance, Sado et al. developed a full lower-limb assistance device for squatting that can reduce the activity of two muscles by 36% [14]. To enable the integration of squat assistance into everyday use in occupational settings, researchers explored the potential benefits of passive or active single-joint devices that assist at the trunk [15–18], hip [19–21], knee [22–28], or ankle [29–31].

The knee joint is particularly crucial during squatting, as it bears the entire body's weight while bending and stabilizing the body. Without proper posture and technique, the knee is especially vulnerable to injury [32, 33]. State-of-the-art studies offer promising knee exoskeleton solutions to benefit wearers with squat assistance. For instance, research demonstrated the potential benefits of knee joint assistance in reducing user energy cost [22] or extensor muscle activities [23, 24] during squatting using various types of tethered devices. Recently, thanks to high compliance and compact quasi-direct drive actuation paradigm, Zhu et al. [25] and Arefeen et al. [26] proposed portable knee exoskeletons can reduce wearers' extensor muscle activities during squatting, demonstrating knee exoskeleton has the potential to benefit users.

However, there is a lack of comprehensive knee exoskeleton studies that meet the multifaceted requirements of squatting assistance, particularly in terms of portability, efficiency, and muscle strain mitigation. While previous knee assistance device studies demonstrate the effectiveness of simple extension assistance in assisting users during squatting, the assisting strategy during the whole squatting cycle (squat-down phase and stand-up phase) with exoskeletons remains inadequately understood. First, most existing exoskeletons are tethered and fixed frames [22–24], unsuitable for work-related scenarios encompassing repositioning. Second, although very preliminary studies suggest the potential for muscle activity reduction during squatting with portable knee exoskeletons [25, 26], it is still uncertain whether and to what extent such a benefit can be effectively achieved. Third, the underlying musculoskeletal effects of knee assistance are still unclear. Specifically, some studies [24, 26] observed reduced muscular activity of extensor muscles when assistance is provided only during the stand-up phase (via positive power), while other studies [22, 23, 25] reported similar muscular activity reduction when assistance is provided during both squat-down (via negative power) and stand-up phases (via positive power). Additionally, the impact of knee assistance during squatting on flexor muscle activity is mixed and remains inconclusive [23, 24, 26].

Addressing these unmet needs requires a comprehensive study of both design and control strategies. In terms of design, Huang et al. proposed a portable knee exoskeleton for walking assistance [34], which shows promise for squat assistance as well, thanks to its lightweight design, high compliance, and wide range of motion. In terms of control, there is still a lack of a generalizable control strategy for assisting different individuals in squatting with various back postures and speeds. In particular, the appropriate assistance strategy for providing negative power at different torque assistance levels during the squat-down phase remains unclear. Specifically, Zhu et al. [25] proposed a stiffness model-based control strategy that provides both negative and positive power during a full squat cycle. Gams et al. [22] proposed an oscillator-based control strategy that performs better than position control and sinewave-based gravity compensation torque control. However, the above assistance strategies do not mimic biologic knee joint torque and overlook the variability of the back postures during squatting, which significantly impacts the torque experienced at the knee joint. Yu et al. [23] proposed a quasi-static model-based knee assistance controller that is biologically relevant to knee moments under various squatting postures. However, it does not consider velocity and acceleration terms, thus not matching knee torques under various squatting speeds. Furthermore, from the subjects' feedback, it emerges that the level of torque assistance is not sufficient during the stand-up phase, while they experience movement restriction during the squat-down phase when the exoskeletons provide higher-level torque assistance.

This study hypothesizes that an untethered, lightweight knee exoskeleton with a generalizable control strategy can reduce muscle activity, enhance efficiency, and decrease perceived exertion during intermittent deep squatting tasks (Fig. 1). This research aims to propose an analytical model-based assistance strategy for a portable knee exoskeleton that enables (1) generalizable squat assistance across various back postures and speeds for different

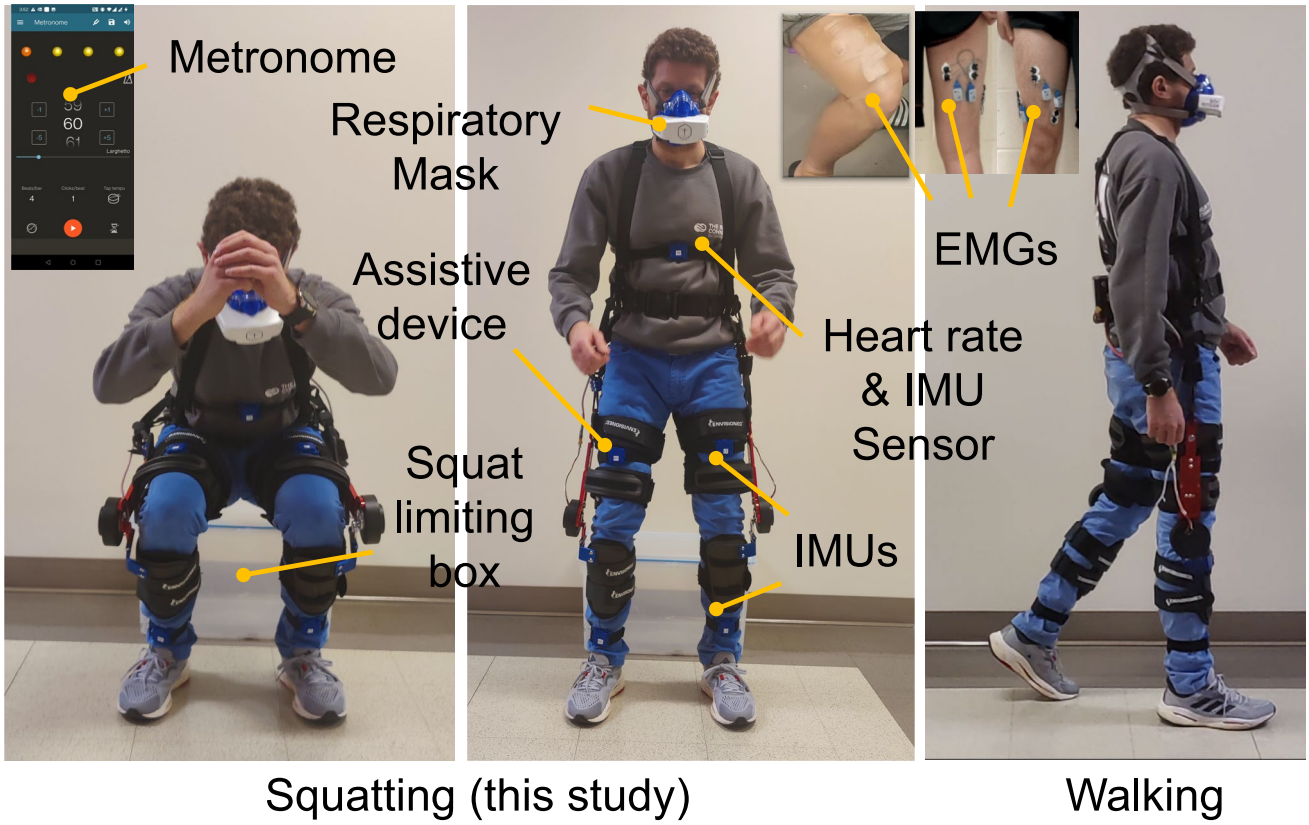

Fig. 1 A simple and generalizable controller for portable knee exoskeletons for squatting assistance aiming to reduce muscle activity (flexors and extensors EMG reduction), enhance user efficiency (metabolic cost, heart rate, and breathing ventilation reduction), or reduce perceived exertion (Borg 6–20 Scale and user preference reduction). The lightweight and portable knee exoskeleton can assist with squatting tasks without restricting walking kinematics.

individuals and (2) precise control over adjustable torque assistance levels during both squat-down and stand-up phases, providing both negative and positive power. Unlike existing studies on active knee exoskeletons for squatting, which did not thoroughly explore the impact of the generalizable assistance strategy across different squat postures, cadences, and individuals characteristics, our work address the multifaceted requirements for squatting assistance in terms of portability, consistent muscle activity reduction (for both flexor and extensor EMG), efficiency enhancement (via reductions in metabolic cost, heart rate, and breathing ventilation), and perceived exertion reduction (assessed through the Borg 6–20 Scale and user preference ranking). Moreover, this study presents a computational musculoskeletal model to analyze knee assistance during squatting. While the majority of the torque assistance is delivered as positive power during the stand-up phase, we investigate the effect of the torque assistance with negative power for three assistance levels during the squat-down phase. Different from the musculoskeletal model predictions that suggest increasing benefits with a higher level of negative power assistance, we find that the best performances are achieved with a moderate level of negative power assistance, followed by no assistance and then high assistance.

Materials and Methods

Portable Knee Exoskeleton for Squatting

The knee exoskeleton aims to provide extension and flexion assistance across a large range of motion. The device is engineered to redistribute musculoskeletal loads away from the knee joint, transferring them to the thigh and shank. This redistribution is designed to diminish the activity of stabilizing muscles, thereby augmenting overall body equilibrium. The exoskeleton's low-profile configuration preserves the natural kinematics of the knee, enabling assisted squatting without constraining the joint's range of motion. This functional integration is achieved through a

lightweight design incorporating integrated quasi-direct drive actuators.

The architecture of the knee exoskeleton encompasses a pair of actuators, a supportive waist belt, onboard control electronics, and a power supply unit. The total mass of the device is 3.5 kg, including the electronics backpack. The actuators utilize quasi-direct drive (QDD) technology, featuring high torque-density motors coupled with low-ratio gearing systems (Fig. 2A) [35–38]. Figure 2B illustrates the intricate mechatronic design. Elastic straps bridge the connection between the thigh support frames and the waist belt, delivering a pretension force that anchors the exoskeleton securely, thereby averting any misalignment between the knee joints and the actuators. The thigh support frame is equipped with an adjustable aluminum linkage on the lateral aspect of the leg, which accommodates two cuffs positioned on the posterior and anterior regions of the thigh. The shank support frame is designed with a single, large anterior cuff and an articulating hinge mechanism that introduces an additional passive degree of freedom, effectively minimizing the potential for knee joint misalignment. This design also permits an unobstructed knee flexion range from 0° to 160°.

Quasi-direct drive (QDD) actuator that harnessing the power of high torque-density motors coupled with low-ratio transmissions, represents a major advancement in wearable robotics [20]. This approach was pioneered in legged robots [39, 40], but it becomes increasingly influential in developing wearable robotics and exoskeleton systems [34–38]. Diverging from our antecedent design that emphasized walking assistance, the present design iteration is meticulously tailored to enhance the torque and power output, thus optimizing it for squatting assistance tasks. The actuator's design incorporates a high torque-density brushless direct current (BLDC) motor (customized Myactuator RMD-X8 series), capable of delivering a peak torque of 6 Nm, integrated with a planetary gear set with a 9:1 ratio. The actuator is lightweight (630 g), compact (98 mm in diameter and 42 mm in height), and has high torque capability (54-Nm peak torque under 20.76-A phase current). The low-ratio transmission yields a reduced output inertia (52.2 kg·cm^2), which is imperative for minimizing impedance to the natural kinematics of the user. The QDD actuator's minimal backdrive torque (0.5 Nm), a consequence of the high torque motor and low gear ratio amalgamation, imparts inherent compliance to the knee exoskeleton, thereby facilitating unencumbered natural movement (Fig. 2C).

The knee exoskeleton's integrated electrical system is encased within a waist belt enclosure and operates on a hierarchical control scheme centered around a Teensy 4.1 microcontroller. This microcontroller executes low-level torque control for the motors alongside tasks, such as sensor signal conditioning, data communication and storage, and power management. The knee joint angles are ascertained using magnetic encoders integrated within the actuators. Notably, low-level torque control accomplished the need for a dedicated torque sensor; rather, it relies on a simplified estimation method that correlates motor current with generated torque, as illustrated in Fig. 2D. The current close-loop PD controller in the low-level control is implemented in the QDD actuator with approximately 20-kHz bandwidth. The overall control bandwidth of the knee exoskeleton is about

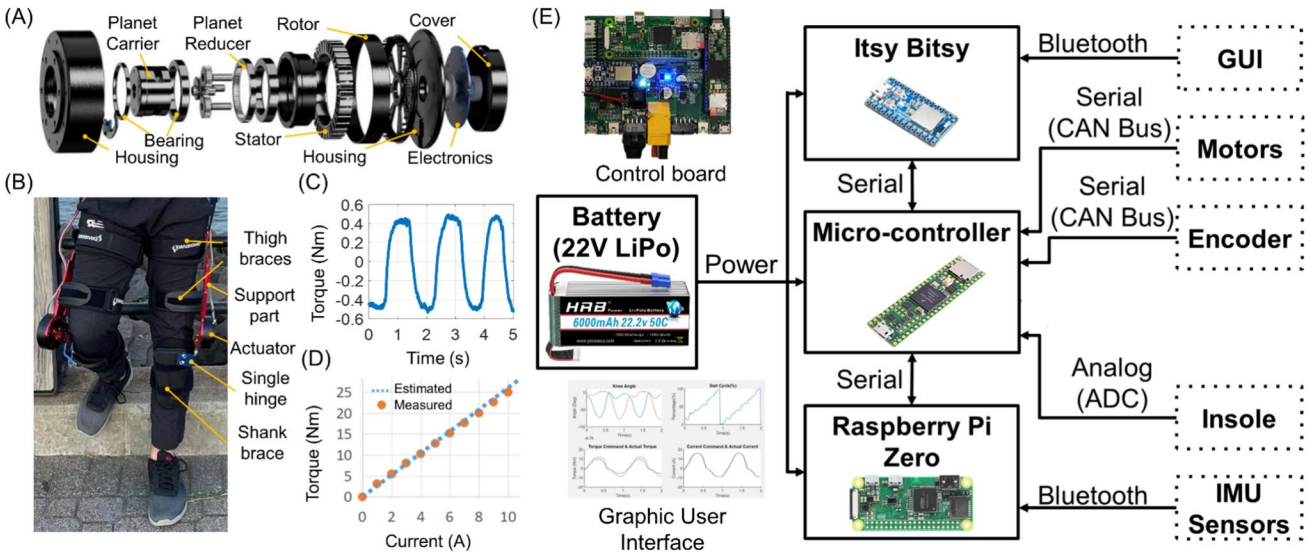

Fig. 2 Mechatronic design of the knee exoskeleton for squatting. **A** Customized quasi-direct drive actuator. **B** Portable knee exoskeleton. **C** Measurement of resistive torque. **D** Measured torque values (dots) alongside the theoretical values derived from the torque constant of the motor (dashed line). **E** Overall electronics schematic

10.8 Hz, which is significantly faster response speed than human 0.5-Hz squatting we studied in this paper. The overall electronics schematics with a customized graphic user interface (MathWorks, USA) are shown in Fig. 2E.

A 22.2 V, 2500 mAh, 270-g lithium-polymer battery serves as the power source and provides an energy capacity P_b of 56 Wh. In the context of a squatting maneuver reaching 90°, the mean net power requirement P_{knee} for an able-bodied individual weighing 70 kg is approximately 336 W [41]. The exoskeleton delivers assistance equivalent to 30% of the biologic torque required for squatting ($k = 0.3$). The assistance protocol prescribes a squatting action completed within 2 s, followed by a 6-s rest period while maintaining a standing posture, resulting in a duty cycle ($\eta = 25\%$). The estimated operational lifespan of the battery T_b can be calculated using (1).

$$T_b = \frac{P_b}{n \times P_{knee} \times k \times \eta}, \tag{1}$$

where $n = 2$ represents two knee joint actuators. The overall battery capacity is able to power the device for 1.1 h (equivalent to providing 500 continuous squatting assistances).

The specification of the portable knee exoskeleton is summarized in Table 1.

Table 1 Portable knee exoskeleton specification

Actuation paradigm	Quasi-direct drive
Weight (kg)	3.5
Gear Ratio	9:1
Nominal Torque (Nm)	18
Peak Torque (Nm)	54
Minimal Backdrive Torque (Nm)	0.5
Range of Motion (°)	0–160
Micro-controller	Teensy 4.1
Battery life (# of squat)	500

Modeling and Control Strategies for Squatting

This section details the modeling and control strategy for squatting assistance, including the human dynamic model for real-time estimates of knee joint torque, a generalizable squat controller, and a computational musculoskeletal biomechanics model for studying the assistance principle.

Human Dynamic Model During Squatting

A multi-segment human biomechanics model is derived to analytically calculate the knee joint torque (Fig. 3). In the model, B is the hip joint, AB segment is the upper body part of the human, C is the knee joint, BC segment is the thigh part of the human, D is the ankle joint, CD segment is the calf part of the human, the lengths of AB, BC, and CD are L_b, L_{th}, and L_{sh}, their corresponding masses are M_b, M_{th}, and M_{sh}, and the angles at the joints are θ_{Tr}, θ_{Th}, and θ_{Sh}. A mathematical coordinate system is established at the ankle (point D) as its origin, and the foot is considered fixed on the ground.

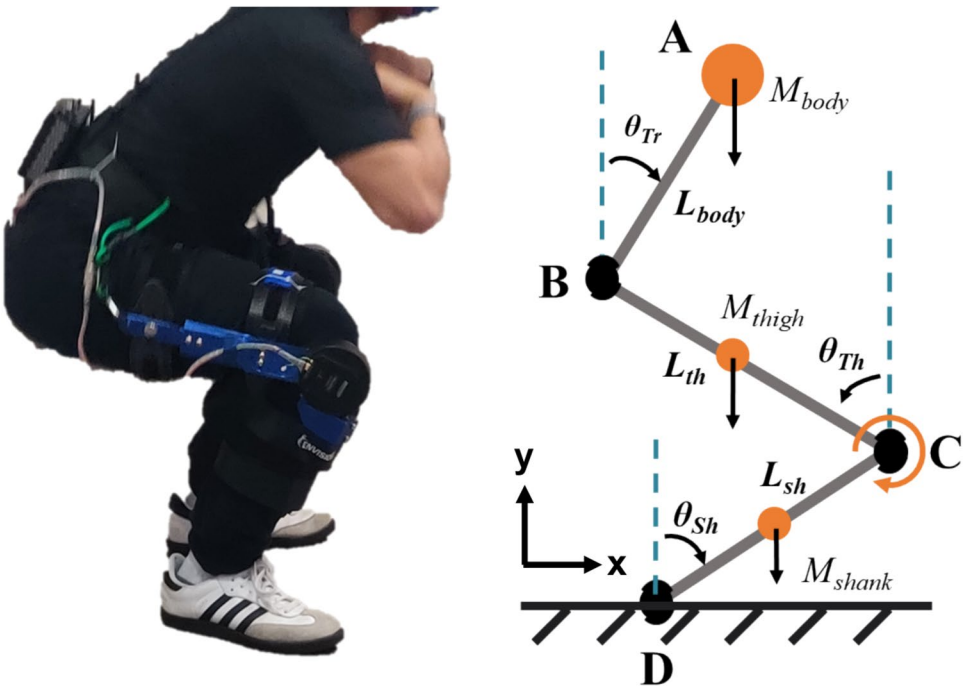

Fig. 3 The analytical biomechanical model for squatting. The annotations denote the combined mass of the upper body (M_{body}), the mass of the thigh (M_{th}), the mass of shank (M_{sh}), the length between the center of mass of M_b and the hip pivot (L_b), the length of the thigh between the hip pivot and knee pivot (L_{th}), the length of the calf between the knee pivot and angle pivot (L_{sh}), the trunk angle (θ_{Tr}), the thigh angle (θ_{Th}), and the shank angle (θ_{Sh}).

Using the Lagrangian method for dynamic analysis, the coordinates of the center of mass (COM) of the segments AB, BC, and CD are solved to determine the change of the COM during motion. The equation derivations are included in the Supplementary Text, and the calculated knee joint moment is expressed as below:

$$\begin{aligned}\tau_{\mathrm{K}} &= \left(M_{\mathrm{b}}L_{\mathrm{sh}}^2 + M_{\mathrm{th}}L_{\mathrm{sh}}^2 + \frac{1}{4}M_{\mathrm{sh}}L_{\mathrm{sh}}^2 + I_3\right)\ddot{\theta}_{\mathrm{Sh}} \\ &- \left(M_{\mathrm{b}}L_{\mathrm{sh}}L_{\mathrm{th}}\cos\theta_{\mathrm{K}} + \frac{1}{2}M_{\mathrm{th}}L_{\mathrm{sh}}L_{\mathrm{th}}\cos\theta_{\mathrm{K}}\right)\ddot{\theta}_{\mathrm{th}} \\ &+ M_{\mathrm{b}}L_{\mathrm{b}}L_{\mathrm{sh}}\cos\left(\theta_{\mathrm{Tr}} - \theta_{\mathrm{Sh}}\right)\ddot{\theta}_{\mathrm{Tr}} - M_{\mathrm{b}}L_{\mathrm{b}}L_{\mathrm{sh}}\sin\left(\theta_{\mathrm{Tr}} - \theta_{\mathrm{Sh}}\right)\dot{\theta}_{\mathrm{Tr}}^2 \\ &+ \left(M_{\mathrm{b}}L_{\mathrm{sh}}L_{\mathrm{th}}\sin\theta_{\mathrm{K}} + \frac{1}{2}M_{\mathrm{th}}L_{\mathrm{sh}}L_{\mathrm{th}}\sin\theta_{\mathrm{K}}\right)\dot{\theta}_{\mathrm{Th}}^2 \\ &- \left(M_{\mathrm{b}} + M_{\mathrm{th}} + \frac{1}{2}M_{\mathrm{sh}}\right)gL_{\mathrm{sh}}\sin\theta_{\mathrm{Sh}}.\end{aligned} \tag{2}$$

Based on Eq. (3), the parameters M_{b}, M_{th}, M_{sh}, L_{b}, L_{th}, and L_{sh} are calculated by data in Table 2 (calculated by data in [42]). This model is customizable because each individual's weight and height can be normalized by M_{w} and L_{H}, respectively. M_{sb} is the mass of the subject, and the L_{sb} is the height of the subject. M_{w} is the total mass of the human model and L_{H} is the total height of the human model from the anthropometry study.

$$\begin{aligned}M_{\mathrm{b}} &= \left(M_{\mathrm{sb}}/M_{\mathrm{w}}\right)\cdot M_1 \\ M_{\mathrm{th}} &= \left(M_{\mathrm{sb}}/M_{\mathrm{w}}\right)\cdot M_2 \\ M_{\mathrm{sh}} &= \left(M_{\mathrm{sb}}/M_{\mathrm{w}}\right)\cdot M_3 \\ L_{\mathrm{b}} &= \left(L_{\mathrm{sb}}/L_{\mathrm{H}}\right)\cdot\left(L_1 - L_5\right) \\ L_{\mathrm{th}} &= \left(L_{\mathrm{sb}}/L_{\mathrm{H}}\right)\cdot\left(L_5 - L_6\right) \\ L_{\mathrm{sh}} &= \left(L_{\mathrm{sb}}/L_{\mathrm{H}}\right)\cdot\left(L_6 - L_4\right)\end{aligned}. \tag{3}$$

Knee Exoskeleton Controller for Squatting

We propose a novel control strategy that provides assistance proportional to the estimated knee joint torque from the above dynamic model, where the assistance levels for the squat-down and stand-up phases are both adjustable. Unlike [21], which used a pre-defined and fixed torque reference was used, our method can provide an adaptive and generic reference torque with biomechanical meaning. In addition, the exoskeleton can provide adjustable torque for both squat-down and stand-up phases based on the detected squat phase. Phase detection is built on the direct measurements of angles and angular velocities from the wearable IMUs. The knee exoskeleton controller can be expressed in (4):

$$\tau_{\mathrm{a}} = \begin{cases} \beta * \alpha * \tau_{\mathrm{K}}, if\, \theta_{\mathrm{K}} < \theta_{\mathrm{Kset}} \& \dot{\theta}_{\mathrm{K}} > \dot{\theta}_{\mathrm{Kset}} \\ \alpha * \tau_{\mathrm{K}}, else \end{cases}, \tag{4}$$

where τ_{K} is the estimated knee joint torque from the dynamic model; α is the exoskeleton assistance level and fixed at 30% in this article; β is a factor expressing the ratio of the squat-down phase assistance level relative to the stand-up phase; and θ_{Th} ($\dot{\theta}_{\mathrm{Th}}$), θ_{Sh} ($\dot{\theta}_{\mathrm{Sh}}$), and θ_{K} ($\dot{\theta}_{\mathrm{K}}$) are the measured angle (angular velocity) of the thigh, shank, and knee joint, respectively. The thigh and shank values are averaged between the left and right sides and measured by four wireless IMU sensors mounted on the subject's bilateral thighs and shanks; θ_{Kset} and $\dot{\theta}_{\mathrm{Kset}}$ are knee joint angle and angular velocity threshold parameters for squat-down phase detection, which are slightly tuned for each subject. $\theta_{\mathrm{Kset}} = 95°$ and $\dot{\theta}_{\mathrm{Kset}} = 30°/\mathrm{s}$ are typical values used in our experiments. A current feedback control guarantees the device's desired torque performance. The overall control schematics are shown in Fig. 4.

Table 2 The human segment parameters

Segment	M_i: Mass (Kg)	L_i: Length between COM to Ground (m)
Upper body	M_1: 52.2 Kg	L_1: 1.20 m
Thighs	M_2: 19.6 Kg	L_2: 0.75 m
Shanks	M_3: 7.6 Kg	L_3: 0.33 m
Feet	M_4: 2 Kg	L_4: 0.028 m
Total	M_W: 81.4 Kg	L_H: 1.784 m
Hip pivot to ground		L_5: 0.946 m
Knee pivot to ground		L_6: 0.505 m

Computational Musculoskeletal Biomechanics Model

To study the biomechanics of squatting and the impact of exoskeleton assistance on muscular loading, we build a 2D musculoskeletal model with idealized torque assistance to the knee joint without explicit modeling of the exoskeleton. The musculoskeletal model is a 2D half-body model with nine major lower-limb muscles on the right side of the body, considering symmetry. These muscles include gluteus maximus (GMAX), iliopsoas (IL), hamstrings (HAMS), rectus femoris (RF), vastus (VAS), biceps femoris short head (BFSH), gastrocnemius (GAS), soleus (SOL), and tibialis anterior (TA). VAS and RF are the knee extensors among these muscles, and BFSH, HAMS, and GAS are the knee flexors. RF and HAM also act to flex and extend the hip, respectively. GAS acts to extend the ankle. The model has 3-DOF planar pelvis joint, 1-DOF lumbar joint, 1-DOF hip, knee, and ankle joints and was adapted from the "gait10dof-18musc" model available within the OpenSim software [43]. The model is constructed in 3D space; however, it is functionally 2D, as all joints are constrained to movement within the sagittal plane kinematically. We created dynamic simulations of squatting with and without knee joint torque

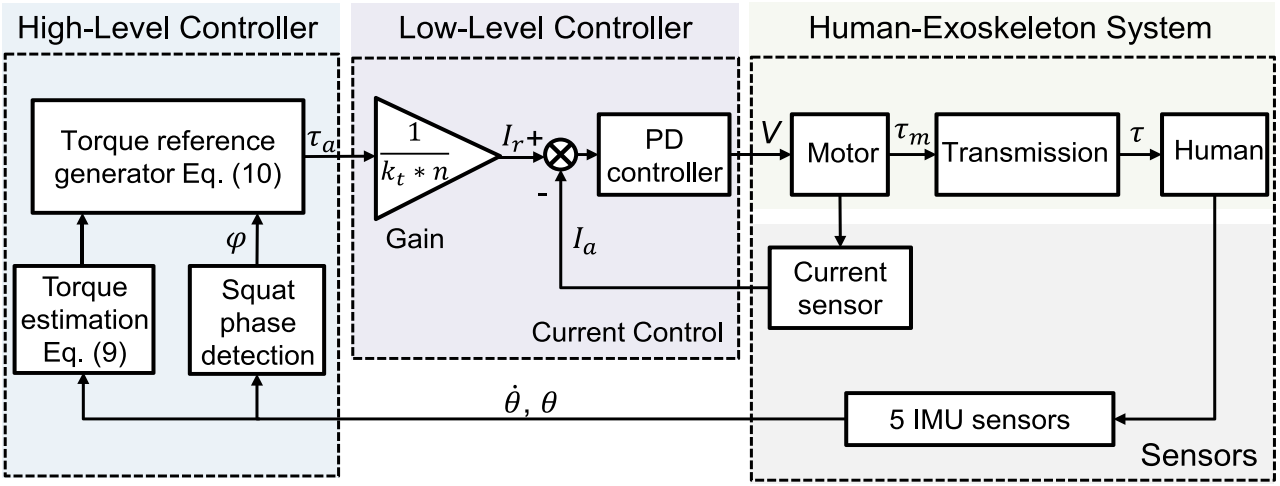

Fig. 4 Schematics of the dynamic analytical model-based control strategy

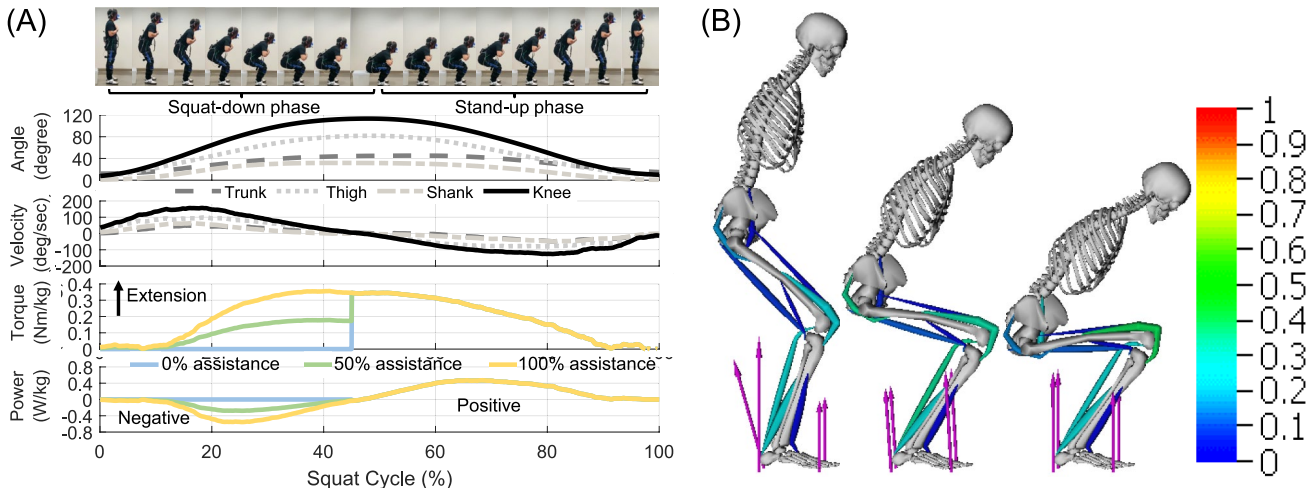

Fig. 5 Computational musculoskeletal biomechanics model driven by experimental data. **A** The mean of measured knee angle and velocity profiles averaged from all conditions and assistance torque and power profiles of a representative subject for each control strategy. **B** Predicted muscle activations during the squat-down phase. The color of the muscles indicates their activation, as shown in the color legend on the right. The arrows represent predicted ground reaction forces at the contact points.

assistance to track the mean hip, knee, and ankle angle profiles shown in Fig. 5A.

The knee assistance torque is set to 30% of the total torque (assistance plus muscle torques) during both the squat-down and squat-up phases. The muscle activations are predicted through optimization, minimizing the sum of squared muscle activations under the constraint of producing the necessary muscle torques. Fig. 5B shows several snapshots of the predicted muscle activations during the squatting cycle. Comparing muscle activations with and without assistance, we found that mean vastus and rectus femoris activations were reduced by 26.7% and 16.7%, respectively. However, the activation of the hamstrings increased by 26.3% during the squat-down phase and 9.4% during the stand-up phase. We further conducted a study with only 15% assistance, and it was observed that hamstring activation was increased only by 4.57% during squat-down. Our simulations suggest that the overall muscle activations can be reduced with proportional torque assistance, but the asymmetric nature of squat-down and stand-up requires further investigation into assistance strategy.

Experiment Setup

The main objective of the experiment is to evaluate the performance of the proposed control strategy for squatting

assistance with a portable knee exoskeleton and systematically study which of the three levels ($\beta = 0, 50\%, 100\%$) of torque assistance strategies during the squat-down phase offers the most benefits. This section details the sensing system integration, outcome measures, protocol, results, and statistical analysis.

Sensing System Integration

We used multiple sensors to evaluate the performance of the proposed system when assisting human squats (Fig. 1). Subjects were asked to squat down with or without the exoskeleton until reaching a box, which was used to fix the lowest squat position. Five wireless IMU sensors were placed on the trunk, thighs, and shanks to measure user kinematics. User cardiorespiratory performance was assessed to demonstrate efficiency enhancement with knee exoskeleton assistance by measuring energy expenditure and breathing ventilation through a respiratory mask (VO2 Master, Canada) and heart rate through a sensing strap (Polar H10, USA). Five wireless EMG sensors (Noraxon Ultium, USA) were placed on five muscles of the subject's right thigh. The overall mechatronics and sensing systems were synchronized, with the IMUs connected to the exoskeleton controller, the EMG sensing system connected to the desktop, and the exoskeleton controller and desktop synchronized through a pair of Bluetooth transceivers (NRF52840, Adafruit, USA) and a customized MATLAB-based graphic user interface (MathWorks, USA). The other sensors were manually synchronized for the respiratory mask and heart rate data. A metronome was also used to guide the subject's squatting frequency during the experiment.

Outcome Measures

For this work, four objective and two subjective metrics were collected during the experiments, including metrics for efficiency enhancement (1. metabolic cost, 2. heart rate, and 3. breathing ventilation), muscle strain mitigation (4. extensor and flexor muscle activity), and user-perceived preference (5. Borg perceived exertion rating and 6. preference ranking). This comprehensive approach ensures a thorough evaluation of the exoskeleton and controller effectiveness.

First, we observed three cardiorespiratory metrics to demonstrate how our knee exoskeleton enhances user efficiency during squatting. Metabolic cost (W/kg), heart rate (bpm), and breathing ventilation (L/min) were recorded and averaged across the last 2 min. The metabolic rates were estimated using the modified Brockway equation [44]. The carbon dioxide volume was derived as proportional to oxygen consumption via the respiratory quotient value (RQ value = 0.85).

The heart rate was normalized based on the formula:

$$\mathrm{HR}_{\mathrm{norm}} = \frac{(\mathrm{HR} - \mathrm{HR}_{\mathrm{rest}})}{(\mathrm{HR}_{\mathrm{max}} - \mathrm{HR}_{\mathrm{rest}})}, \tag{5}$$

where HR was the average heart rate measured in the last 2 min, $\mathrm{HR}_{\mathrm{rest}}$ was the rest heart rate, and $\mathrm{HR}_{\mathrm{max}}$ was the maximum heart rate estimated as a function of the wearer's age using the equation [45]:

$$\mathrm{HR}_{\mathrm{max}} = 206.9 - 0.67 \times \mathrm{age}. \tag{6}$$

Second, we observed muscle activity as a metric to evaluate exoskeleton assistance's effectiveness in mitigating muscle strain. Five major muscles of the right thigh acting on the knee joint during squatting (two flexors and three extensors) were collected at 1000 Hz for analysis: vastus lateralis (VL), rectus femoris (RF), vastus medialis (VM), biceps femoris (BF), and semitendinosus (SEM). We implemented several measures to minimize the impact of motion artifacts on EMG measurements. First, we used a differential measurement scheme with three electrodes for EMG measurement. For each EMG sensor, two recording electrodes were placed in the area fully covered by the upper thigh straps, and the reference electrode was placed in the space between the two thigh straps. Second, all the electrodes were fixed with stretchable elastic compression bandages to reduce the displacement and irregular extrusion of the sensor caused by user movement and human–exoskeleton interaction. Third, we instructed the subjects to keep their limbs relaxed and mentally focused during the experiment to avoid unnecessary movements. Fourth, the raw EMG data were notch filtered with a band-stop filter (58–62 Hz, 4th-order, zero-phase Butterworth filter) and a bandpass filter (30–500 Hz, 4th-order, zero-phase Butterworth filter). For each muscle, the root mean square (RMS) and maximum (Max) of the EMG signal were extracted for five squats, averaged and then normalized to the RMS or peak in all five averaged conditions. We normalized the RMS and peak values across seven subjects. For visualization, the time series data were filtered by a low-pass filter (20 Hz, 4th-order, zero-phase Butterworth filter), normalized to 1000 data points, and averaged across five squat cycles. The primary intention of the knee exoskeleton assistance during squatting was not only to replace a portion of the biologic effort of the knee extensor muscles during the extension phase but also to enhance overall body balance by supporting both extensor and flexor muscles, which were used for stabilization. We averaged 35 squat cycles (5 for each of the seven subjects). We observed the average amplitude of RMS EMG in five muscles (three knee extensors and two knee flexors) under the five conditions to understand the assistive effect.

Third, after finishing each condition, the subject was asked to assess the perceived exertion level using the Borg 6–20 RPE scale. Before the experiments, participants were thoroughly instructed on the Borg rating of perceived exertion. At the end of the test, the subjects were asked to rank the conditions that require the least physical effort (Rank 1 indicates the preferred condition).

Experimental Protocol and Statistical Analysis

Since workers require squatting under different angles, cadences, and loads in various industrial scenarios, it is difficult to conduct one universal controlled experiment to fit all such situations. In this study, inspired by previous squatting assistance studies using ankle exoskeletons [29, 30], we chose a controlled laboratory experiment with fixed squat angles and cadence and no external load. This allows us to isolate the effects of different knee assistance strategies provided by a portable knee exoskeleton during repetitive squatting. Specifically, seven able-bodied subjects (female = 2, age: 23.0 ± 1.0 years, height: 171.0 ± 2.9 cm, mass: 69.4 ± 4.6 kg, mean ± standard deviation) provided written informed consent to participate in the following experiment approved by the NC State University Institutional Review Board (eIRB # 24675). The torque assistance level was set to 30% of the estimated biologic knee torque (normalized by the height and mass for each subject) based on Eqs. (9)–(11). We designed and implemented a two-session protocol to evaluate the developed system. The assistance torque during the squat-down cycle was equivalent to 0% (zero-torque control to compensate motor backdrive torque during squatting), 50%, and 100% of the assistance level during the stand-up cycle (30% of the estimated biologic knee torque), as shown in Fig. 5A. In the unpowered condition, the subjects wore the exoskeleton, while it was turned off (no zero-torque control for compensation). The first visit was for exoskeleton fitting, control tuning, and adaptation to the assistance of different controllers. We tuned and adjusted the exoskeleton to fit the subject best. The subject then squatted at least ten times in each of the five conditions (baseline, unpowered, 0% assistance, 50% assistance, and 100% assistance). We randomized the order of the conditions to minimize the learning effect. In the powered conditions, the exoskeleton provided assistance torque equivalent to 0%, 15%, and 30% of the estimated biologic knee torque during the squat-down phase and 30% during the stand-up phase. The resting metabolic rates were measured at the beginning of the second visit. Then, the subject performed squatting tests under five conditions while we recorded data. We randomized the order of the conditions to prevent bias in the data collection. Following similar human evaluation studies [30], the subject squatted for 4 min under each condition. The squat cycle comprised 1-s squat-down, 1-s stand-up, followed by 6 s of rest. The subject fully rested for at least 15 min between two consecutive tests. We processed the data and conducted statistical analyses in MATLAB. A paired t test with Holm–Bonferroni correction was used to determine if quantitative differences exist in squat conditions (significance level $p < 0.05$). RMS ± Standard Error of the Mean (SEM, marked as error bars) of the net metabolic cost, normalized heart rate, ventilation, RMS, and Max of each muscle activity change between wearing exoskeleton (unpowered, 0% assistance, 50% assistance, and 100% assistance) and baseline conditions were calculated. Asterisks indicate that the changes are statistically significant compared with the baseline.

Results

Efficiency Quantified Via Metabolic Cost, Heart Rate, and Breathing Ventilation

Across all subjects, all assistance conditions showed reduced the heart rate, and ventilation of subjects compared to the unpowered and baseline conditions, while metabolic cost, heart rate, and ventilation of subjects increased in the unpowered condition compared to the baseline condition (Fig. 6). In detail, in the unpowered condition metabolic cost increased by 7.4 ± 2.6%, heart rate by 7.0 ± 2.7%, and ventilation by 5.7 ± 1.4%; in the 0% assistance condition metabolic cost was reduced by 10.3 ± 3.3%, heart rate by 14.5 ± 3.8%, and ventilation by 8.1 ± 2.3%; in the 50% assistance condition metabolic cost was reduced by 12.8 ± 2.8%, heart rate by 13.8 ± 3.0%, and ventilation by 8.9 ± 3.0%; in the 100% assistance condition metabolic cost was reduced by 2.6 ± 2.2%, heart rate by 5.4 ± 2.7%, and ventilation by 1.0 ± 4.4%.

Muscle Strain Mitigation Quantified Via EMG

Figure 7A shows that the extensor muscle group activities were reduced under all three assistance conditions, while the flexor muscle group activities were not statistically changed. The unpowered condition's amplitude was slightly higher than the baseline. The changes in the four (assisted and unassisted) conditions compared to the RMS and Max EMG baseline are reported in Fig. 7B and Table 3.

User Preference Quantified Via Borg-Perceived Exertion Scales and Preference Ranking

Across all subjects, all seven subjects perceived less muscle effort with exoskeleton assistance compared to both the unpowered and baseline conditions. Three of them also reported the feeling of undesirable resistance during the squat-down cycle using the 100% assistance control strategy.

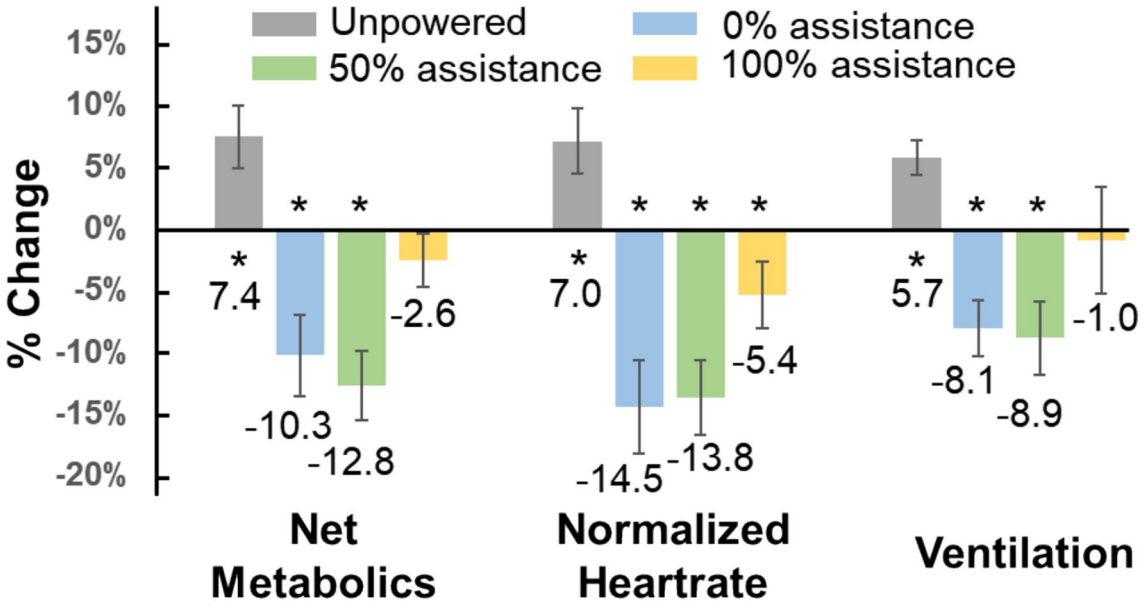

Fig. 6 Efficiency enhancement results in terms of metabolic cost, heart rate, and breathing ventilation. Average changes in net metabolic cost, normalized heart rate, and ventilation in assisted and non-assisted conditions compared to baseline conditions across all subjects ($n=7$). For every assistance condition, all three metrics were lower than the baseline condition, demonstrating the efficiency enhancement of the knee exoskeleton for squatting.

The average RPE scores were 12.43 ± 0.53 (baseline), 13.00 ± 0.44 (unpowered), 10.86 ± 0.59 (0% assistance), 10.57 ± 0.48 (50% assistance), and 11.29 ± 0.42 (100% assistance), respectively (Fig. 8A). The perceived exertion reduction in the three assist-on conditions ranged from 1 to 3. All except one subject ranked the unpowered condition as the most physically demanding (Fig. 8B). Among the three assistance strategies, most subjects preferred 0% or 50% assistance. In particular, 50% assistance received the best score. Subjects' ranks relative to the 100% assistance strategy were very scattered. One participant commented that he could feel significant assistance during the squat-down phase. At the same time, another reported significant resistance, and the others provided positive feedback but with lower appreciation than the other assistance strategies.

Discussion

The results of the proposed analytical model-based control strategies demonstrated that our portable knee exoskeleton can enhance user efficiency (reduce metabolic cost, heart rate, and breathing ventilation) and muscle strain mitigation (reduce muscle activity) during squatting tasks. Subjective feedback from the participants further supports these findings, as they reported reduced perceived exertion and ranked the assistance conditions higher than baseline and unpowered conditions. Together, these results validate the device's effectiveness in assisting squatting.

While most participants generally benefited from all three tested assistance strategies, the most benefit was achieved with a moderate (50% assistance) level of torque assistance during the squat-down phase, followed by the controller without assistance (0% assistance), and then the high-level assistance (100% assistance), in terms of most objective and subjective metrics except for heart rate. In particular, the overall knee flexor muscle activity reduction was only reported under the controller with a moderate-level assistance condition. Interestingly, the overall preference ranking among the three levels of assistance control strategies did not fully align with predictions from human musculoskeletal model analyses but resonated with subject feedback. The results in Table 3 indicate that knee extension torque assistance effectively diminished the activation of the knee extensor muscle group across all three assistance conditions during the stand-up phase, aligning with the musculoskeletal analysis of human exoskeleton models. Conversely, during the squat-down phase, the model suggested that with increasing assistance levels (up to 30% of biologic torque), the activities of the human extensor muscle group decreased while the activities of the flexor muscle group increased. Specifically, during the squat-down phase, the 0% assistance-level control strategy did not change the users' flexor and extensor muscle activities, the 50% assistance-level control strategy reduced the users both flexor and extensor muscle activities, and 100% assistance-level control strategy only reduced user extensor muscle activities and increased flexor muscle activities. We posited that this inconsistency

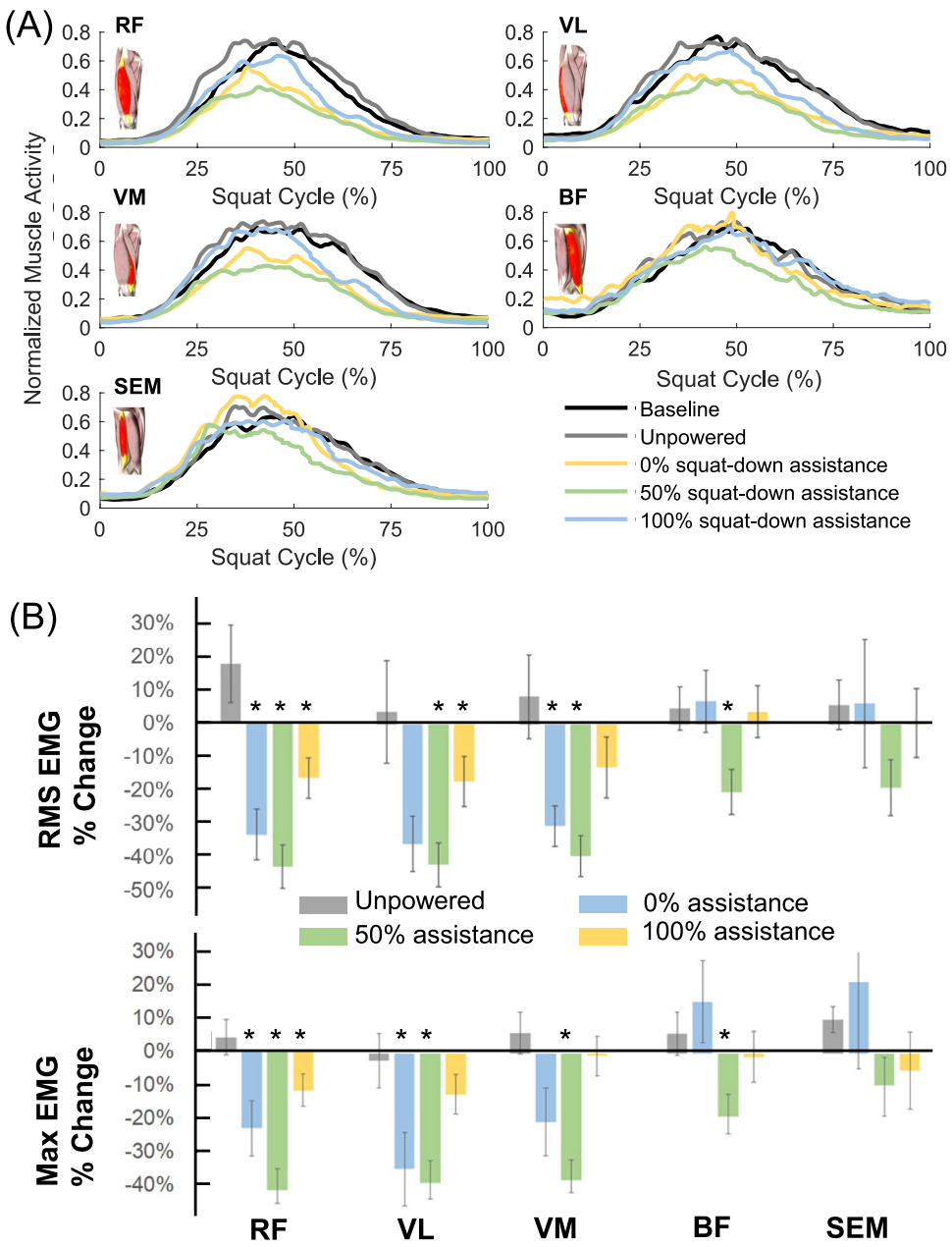

Fig. 7 Muscle strain mitigation results in terms of EMG. **A** Averaged activity of three extensors (RF, VL, VM) and two flexor (BF, SEM) muscles under different test conditions (baseline, unpowered, 0% squat-down assistance, 50% squat-down assistance, 100% squat-down assistance) across all subjects ($n = 7$). The results showed that the exoskeleton with all three assistance strategies effectively reduced the activities of the three extensor muscles. **B** Changes in normalized RMS and Max EMG averaged across five squat cycles and all the subjects ($n = 7$) in assisted and non-assisted conditions compared to baseline. The results showed that exoskeleton with moderate (50% assistance) level torque assistance strategies effectively reduced the activities of both extensor (RMS reduction of 39.39–43.22%) and flexor (RMS reduction of 18.89–20.25%) muscles.

may stem from the exoskeleton providing suitable extension assistance during the squat-down phase, enabling users to enhance movement stability, thereby concurrently reducing the activities of the relevant extensor and flexor muscle groups. However, excessive extension assistance may impede users, leading them to exert greater muscle effort to complete the action. This greater muscle effort could be due to the user's lack of adaptation to large external assistance or the non-ideal human–exoskeleton interaction. Another potential reason is that the large external assistance from wearable robots reduces user comfort or makes them feel a fear of stability loss, particularly during the 100% squat-down assistance condition. Notably, these effects vary among individuals, underscoring the need for personalized assistance strategies in the design of knee exoskeletons. Another plausible reason for the inconsistency between motion prediction and experimental findings could be individuals' level of muscle co-contraction during different assistance levels. The model aims to reduce overall muscle activations and diminish muscle co-contraction, whereas, in the experiment, subjects may employ different levels of muscle co-contraction for perceived stability and comfort during assistance, especially at high levels of assistance. Beyond the specific application of squatting, we believe these insights could also apply to other controllers designed for multifaceted tasks. Such tasks may require the judicious application

Table 3 Comparison of the RMS and max EMG among different conditions vs. baseline—seven-subject group results

vs. Baseline (%)	RF	VL	VM	BF	SEM
Unpowered					
Max (full squat)	4.4	−2.1	6.2	5.9	10.3
Mean (full squat)	17.7	3.8	8.4	4.9	5.9
Mean (squat-down only)	19.9	6.7	14.0	13.8	10.8
Mean (squat-up only)	14.7	0.6	2.0	−3.9	−0.1
0% squat-down assistance					
Max (full squat)	−11.6	−12.2	−0.7	−1.0	−5.0
Mean (full squat)	−16.6	−17.1	−12.8	3.9	0.5
Mean (squat-down only)	−4.2	−5.4	4.8	5.9	9.0
Mean (squat-up only)	−33.3	−29.8	−33.0	2.0	−9.9
50% squat-down assistance					
Max (full squat)	−41.7	−38.8	−38.1	−18.9	−9.5
Mean (full squat)	−43.2	−42.1	−39.4	−20.2	−18.9
Mean (squat-down only)	−34.5	−34.0	−30.2	−7.1	−2.4
Mean (squat-up only)	−55.0	−50.9	−50.0	−33.1	−39.2
100% squat-down assistance					
Max (full squat)	−23.0	−34.7	−20.5	15.7	21.6
Mean (full squat)	−33.6	−35.8	−30.4	7.0	6.3
Mean (squat-down only)	−25.5	−31.6	−22.4	26.6	29.9
Mean (squat-up only)	−44.4	−40.4	−39.7	−12.2	−22.6

of negative power from assistive devices, including kneeling, stooping, or transitioning from standing to sitting.

There are several limitations to this study. Firstly, the proposed control strategy is not individually optimized for each subject. Online [30] and offline [46] optimization algorithms can be used to provide personalized assistance, potentially improving assistance performance further. Secondly, while the results in this article demonstrate the feasibility and effectiveness of squat assistance in enhancing efficiency and reducing muscle activities, it is important to acknowledge that all experiments were conducted with healthy subjects in a controlled setting. Evaluating the assistance of professional workers at actual occupational sites yield more referenceable insights.

In summary, this article presents a simple and generalizable torque controller for a portable knee exoskeleton that can independently control negative (squat-down phase) and positive power (stand-up phase) for squatting assistance. Compared with the state-of-the-art studies using active knee exoskeletons to assist squatting, where the impact of the generalizable assistance strategy (for different squat postures, cadences, and individuals) is not extensively studied, our work tackled the multifaceted requirements for squatting assistance in terms of portability, consistent effectiveness for muscle strain mitigation (muscle activity), efficiency

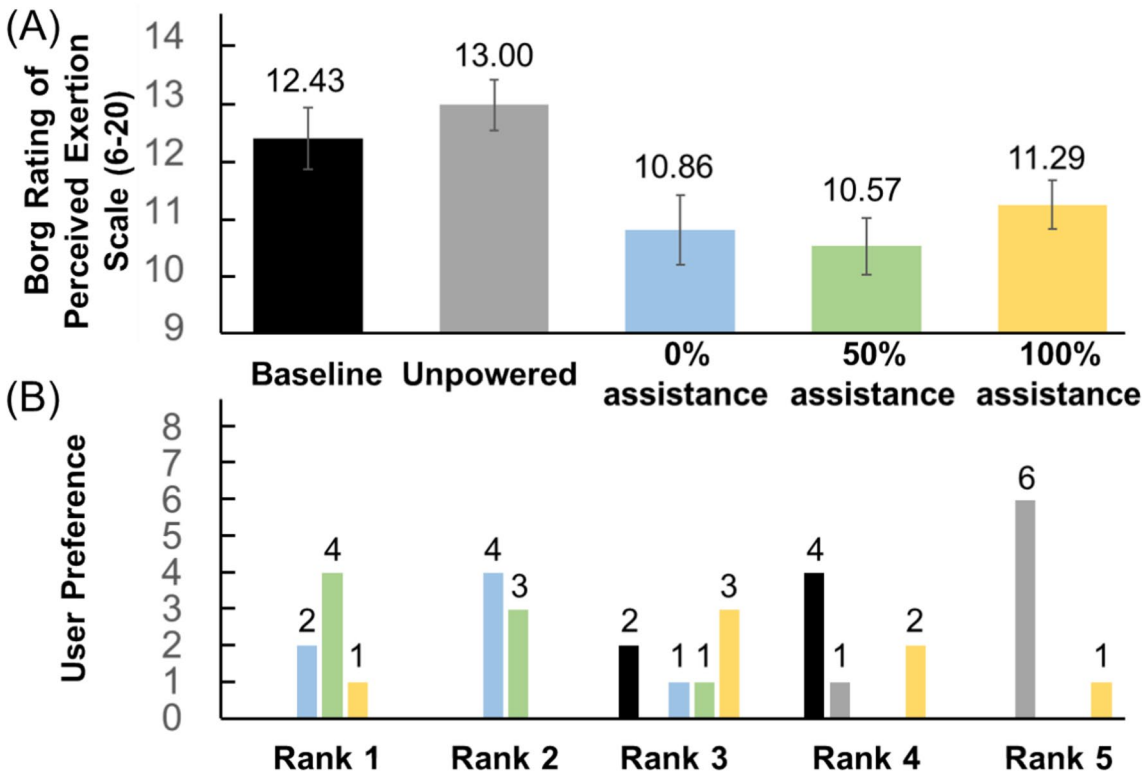

Fig. 8 Two subjective evaluation metrics were used to collect subjects' feedback about each test condition ($n = 7$). **A** Averaged perceived exertion was measured by the Borg 6–20 RPE scale across subjects. **B** The distribution of user preference ranks (rank 1 indicates the preferred condition)

Table 4 Study results comparison of active knee exoskeleton for squatting

Study[1, 2]	JSI [22]	CCNY [23]	ASU [24]	UMich [25]	OSU [26]	Ours		
Device Type	Tethered	Tethered	Tethered	Portable	Portable	Portable		
Assist phase	Full squat	Full squat	Stand-up	Full squat	Stand-up	0% assist[3]	50% assist[3]	100% assist[3]
# of Subject	**7**	3	8	3	3	7		
Energy cost	22.7% ↓ *	N/A	N/A	N/A	N/A	10.3% ↓ *	**12.8%** ↓ *	2.6% ↓
Heart rate	33.6% ↓ *					14.5% ↓ *	**13.8%** ↓ *	5.4% ↓ *
Breathing ventilation	27.2% ↓ *					8.1% ↓ *	**8.9%** ↓ *	1.0% ↓
EMG Extensor (s)	Inconclusive	75 ~ 87.5% ↓	55% ↓ *	19.3 ~ 31.8% ↓	35.3 ~ 57.8% ↓	12.8 ~ 16.6% ↓ *	**39.4 ~ 43.2%** ↓ *	30.4 ~ 35.7% ↓ *
EMG Flexor (s)	N/A	Slightly increased ↑	Inconclusive	N/A	28.9% ↓	0.5 ~ 3.0% ↑	**18.9 ~ 20.3%** ↓ *	6.3–7.0%↓
Borg 6–20 scales	N/A	N/A	N/A	N/A	N/A	1.5 ↓	**1.8** ↓	0.1 ↓

Bold values indicate the best performance among the three assistance strategies

[1]Compared to not wearing an exoskeleton, ↓ means better

[2]Asterisks indicate statistical significance compared with the baseline ($p < 0.05$)

[3]Only different in the squat-down assistance phase

enhancement (metabolic cost, heart rate, breathing ventilation), and perceived exertion reduction (Borg 6–20 Scale and user preference), as shown in Table 4. The proposed method can significantly assist squatting consistently with the above four objective and two subjective metrics. Experimental results with seven able-bodied subjects demonstrated the effectiveness of our exoskeleton, which was able to reduce metabolic cost by 12.8%, heart rate by 13.8%, breathing ventilation by 8.9%, extensor muscle activity by 39.4–43.2%, flexor muscle activity by 18.9–20.3%, and 1.8 Borg perceived exertion scale, compared to the baseline condition of not wearing the exoskeleton. The human subject testing results show the proposed knee exoskeleton has the potential to reduce muscle strain and enhance working efficiency during squatting-related tasks for workers. Future studies could investigate the effects of multiple different control strategies, such as simple on-off, gravity compensation, scaled biologic torque, and dynamic model-based controllers, in real occupational working scenarios.

Supplementary Information The online version contains supplementary material available at https://doi.org/10.1007/s10439-025-03696-0.

Acknowledgments S. Yu, S. Zhang, A. Di Lallo, J. Zhu, and H. Su were supported in part by the National Science Foundation CAREER award CMMI 1944655, NSF Future of Work 2231419, NSF Cyber-Physical System 2344956, Switzer Distinguished Fellow SFGE22000372 of the National Institute on Disability, Independent Living, and Rehabilitation Research (NIDILRR). This work was performed at NCSU when S. Yu was a postdoctoral fellow at NCSU. S. Zhang, A. Di Lallo, J. Zhu, and H. Su had no financial support other than stated here. S. Yu, L. Liu, Q. Wu, and G. Zuo were supported in part by the National Nature Science Foundation of China (62373016, 62403020) and the Open Projects Program of State Key Laboratory of Multimodal Artificial Intelligence Systems (MAIS-2023-22). X. Zhou is supported in part by a Centers for Disease Control and Prevention (CDC)/National Institute for Occupational Safety & Health (NIOSH) Grants (75D30120P08812, 75D30123P17823).

Declarations

Conflict of interest The authors declare that they have no known competing financial interests or personal relationships that could have appeared to influence the work reported in this paper. All research was conducted at North Carolina State University and approved by the NC State University Institutional Review Board (eIRB # 24675).

Citation Diversity Statement Recent work in several fields of science has identified a bias in citation practices such that papers from women and other minority scholars are under-cited relative to the number of papers in the field. We recognize this bias and have worked diligently to ensure that we are referencing appropriate papers with fair gender and racial author inclusion.

References

1. Palmer, K. T. Occupational activities and osteoarthritis of the knee. *Br. Med. Bull.* 102(1):147–170, 2012.
2. Howard, J., V. V. Murashov, B. D. Lowe, and M. L. Lu. Industrial exoskeletons: need for intervention effectiveness research. *Am. J. Ind. Med.* 63(3):201–208, 2020.
3. Kim, S., A. Moore, D. Srinivasan, A. Akanmu, A. Barr, C. Harris-Adamson, D. M. Rempel, and M. A. Nussbaum. Potential of exoskeleton technologies to enhance safety, health, and performance in construction: industry perspectives and future

research directions. *IISE Tran. Occup. Ergon. Hum. Factors*. 7(3–4):185–191, 2019.
4. Amin, S., J. Goggins, J. Niu, A. Guermazi, M. Grigoryan, D. J. Hunter, H. K. Genant, and D. T. Felson. Occupation-related squatting, kneeling, and heavy lifting and the knee joint: a magnetic resonance imaging-based study in men. *J. Rheumatol.* 35(8):1645–1649, 2008.
5. Luo, S., M. Jiang, S. Zhang, J. Zhu, S. Yu, I. Dominguez Silva, T. Wang, E. Rouse, B. Zhou, H. Yuk, X. Zhou, and H. Su. Experiment-free exoskeleton assistance via learning in simulation. *Nature*. 630(8016):353–359, 2024.
6. Di Lallo, A., S. Yu, J. E. Slightam, G. X. Gu, J. Yin, and H. Su. Untethered fluidic engine for high-force soft wearable robots. *Adv. Intell. Syst.* 2024. https://doi.org/10.1002/aisy.202400171.
7. Xing, X., S. Zhang, T. Huang, J. S. Huang, H. Su, and Y. Li. Spatial iterative learning torque control of robotic exoskeletons for high accuracy and rapid convergence assistance. *IEEE/ASME Trans. Mechatron.* 2024. https://doi.org/10.1109/TMECH.2024.3365045.
8. Zhang, S., J. Zhu, T.-H. Huang, S. Yu, J. S. Huang, I. Lopez-Sanchez, T. Devine, M. Abdelhady, M. Zheng, and T. C. Bulea. Actuator optimization and deep learning-based control of pediatric knee exoskeleton for community-based mobility assistance. *Mechatronics*. 97:103109, 2024.
9. Ranaweera, R., R. Gopura, T. Jayawardena, and G. K. Mann. Development of a passively powered knee exoskeleton for squat lifting. *J. Robot. Netw. Artif. Life*. 5(1):45–51, 2018.
10. Yan, Z., B. Han, Z. Du, T. Huang, O. Bai, and A. Peng. Development and testing of a wearable passive lower-limb support exoskeleton to support industrial workers. *Biocybern. Biomed. Eng.* 41(1):221–238, 2021.
11. Alemi, M. M., S. Madinei, S. Kim, D. Srinivasan, and M. A. Nussbaum. Effects of two passive back-support exoskeletons on muscle activity, energy expenditure, and subjective assessments during repetitive lifting. *Hum. Factors*. 62(3):458–474, 2020.
12. Tu, Y., A. Zhu, J. Song, X. Zhang, and G. Cao. Design and experimental evaluation of a lower-limb exoskeleton for assisting workers with motorized tuning of squat heights. *IEEE Trans. Neural Syst. Rehabil. Eng.* 30:184–193, 2022.
13. Wang, Z., X. Wu, Y. Zhang, C. Chen, S. Liu, Y. Liu, A. Peng, and Y. Ma. A semi-active exoskeleton based on EMGs reduces muscle fatigue when squatting. *Front. Neurorobot.* 15:625479, 2021.
14. Sado, F., H. J. Yap, R. A. R. Ghazilla, and N. Ahmad. Design and control of a wearable lower-body exoskeleton for squatting and walking assistance in manual handling works. *Mechatronics*. 63:102272, 2019.
15. Poon, N., L. van Engelhoven, H. Kazerooni, and C. Harris. Evaluation of a trunk supporting exoskeleton for reducing muscle fatigue. In: Proceedings of the Human Factors and Ergonomics Society Annual Meeting. Los Angeles: SAGE, 2019, pp. 980–983.
16. Baltrusch, S., J. Van Dieën, S. Bruijn, A. Koopman, C. Van Bennekom, and H. Houdijk. The effect of a passive trunk exoskeleton on metabolic costs during lifting and walking. *Ergonomics*. 62:903–916, 2019.
17. Huysamen, K., M. de Looze, T. Bosch, J. Ortiz, S. Toxiri, and L. W. O'Sullivan. Assessment of an active industrial exoskeleton to aid dynamic lifting and lowering manual handling tasks. *Appl. Ergon.* 68:125–131, 2018.
18. Ding, S., F. A. Reyes, S. Bhattacharya, A. Narayan, S. Han, O. Seyram, and H. Yu. A novel back-support exoskeleton with a differential series elastic actuator for lifting assistance. *IEEE Trans. Robot.* 2023. https://doi.org/10.1109/TRO.2023.3331680.
19. Wei, W., S. Zha, Y. Xia, J. Gu, and X. Lin. A hip active assisted exoskeleton that assists the semi-squat lifting. *Appl. Sci.* 10(7):2424, 2020.
20. Yu, S., T.-H. Huang, X. Yang, C. Jiao, J. Yang, Y. Chen, J. Yi, and H. Su. Quasi-direct drive actuation for a lightweight hip exoskeleton with high backdrivability and high bandwidth. *IEEE/ASME Trans. Mechatron.* 25(4):1794–1802, 2020.
21. Chen, B., L. Grazi, F. Lanotte, N. Vitiello, and S. Crea. A real-time lift detection strategy for a hip exoskeleton. *Front. Neurorobot.* 12:17, 2018.
22. Gams, A., T. Petrič, T. Debevec, and J. Babič. Effects of robotic knee exoskeleton on human energy expenditure. *IEEE Trans. Biomed. Eng.* 60(6):1636–1644, 2013.
23. Yu, S., T.-H. Huang, D. Wang, B. Lynn, D. Sayd, V. Silivanov, Y. S. Park, Y. Tian, and H. Su. Design and control of a high-torque and highly backdrivable hybrid soft exoskeleton for knee injury prevention during squatting. *IEEE Robot. Autom. Lett.* 4(4):4579–4586, 2019.
24. Yumbla, E. Q., S. Sridar, and W. Zhang. Evaluating the benefits of a soft inflatable knee exosuit during squat lifting. In: Proc 2022 9th IEEE RAS/EMBS International Conference for Biomedical Robotics and Biomechatronics (BioRob). IEEE, pp. 1–7.
25. Zhu, H., C. Nesler, N. Divekar, V. Peddinti, and R. D. Gregg. Design principles for compact, backdrivable actuation in partial-assist powered knee orthoses. *IEEE/ASME Trans. Mechatron.* 26(6):3104–3115, 2021.
26. Arefeen, A., and Y. Xiang. A comparative analysis of optimal and biomechanical torque control strategies for powered knee exoskeletons in squat lifting. *J. Mech. Robot.* 2023. https://doi.org/10.1115/1.4064234.
27. Yu, S., T.-H. Huang, A. Di Lallo, S. Zhang, T. Wang, Q. Fu, and H. Su. Bio-inspired design of a self-aligning, lightweight, and highly-compliant cable-driven knee exoskeleton. *Front. Hum. Neurosci.* 16:1018160, 2022.
28. Chen, S., D. T. Stevenson, S. Yu, M. Mioskowska, J. Yi, H. Su, and M. Trkov. Wearable knee assistive devices for kneeling tasks in construction. *IEEE/ASME Trans. Mechatron.* 26(4):1989–1996, 2021.
29. Jeong, H., P. Haghighat, P. Kantharaju, M. Jacobson, H. Jeong, and M. Kim. Muscle coordination and recruitment during squat assistance using a robotic ankle–foot exoskeleton. *Sci. Rep.* 13(1):1363, 2023.
30. Kantharaju, P., H. Jeong, S. Ramadurai, M. Jacobson, H. Jeong, and M. Kim. Reducing squat physical effort using personalized assistance from an ankle exoskeleton. *IEEE Trans. Neural Syst. Rehabil. Eng.* 30:1786–1795, 2022.
31. Ramadurai, S., M. Jacobson, P. Kantharaju, H. Jeong, H. Jeong, and M. Kim. Evaluation of lower limb exoskeleton for improving balance during squatting exercise using center of pressure metrics. In: Proceedings of the Human Factors and Ergonomics Society Annual Meeting. Los Angeles: SAGE, pp. 858–862.
32. Escamilla, R. F. Knee biomechanics of the dynamic squat exercise. *Med. Sci. Sports Exerc.* 33(1):127–141, 2001.
33. Neumann, D. A. Kinesiology of the Musculoskeletal System: Foundations for Rehabilitation, 3rd Edition. Mosby Elsevier, 2016.
34. Huang, T.-H., S. Zhang, S. Yu, M. K. MacLean, J. Zhu, A. Di Lallo, C. Jiao, T. C. Bulea, M. Zheng, and H. Su. Modeling and stiffness-based continuous torque control of lightweight quasi-direct-drive knee exoskeletons for versatile walking assistance. *IEEE Trans. Robot.* 2022. https://doi.org/10.1109/TRO.2022.3170287.
35. Zhu, J., C. Jiao, I. Dominguez, S. Yu, and H. Su. Design and backdrivability modeling of a portable high torque robotic knee prosthesis with intrinsic compliance for agile activities. *IEEE/ASME Trans. Mechatron.* 27(4):1837–1845, 2022.
36. Lee, D., B. J. McLain, I. Kang, and A. J. Young. Biomechanical comparison of assistance strategies using a bilateral robotic knee exoskeleton. *IEEE Trans. Biomed. Eng.* 68(9):2870–2879, 2021.

37. Lee, D., E. C. Kwak, B. J. McLain, I. Kang, and A. J. Young. Effects of assistance during early stance phase using a robotic knee orthosis on energetics, muscle activity, and joint mechanics during incline and decline walking. *IEEE Trans. Neural Syst. Rehabil. Eng.* 28(4):914–923, 2020.
38. Rodríguez-Jorge, D., S. Zhang, J. S. Huang, I. Lopez-Sanchez, N. Srinivasan, Q. Zhang, X. Zhou, and H. Su. Biomechanics-informed mechatronics design of comfort-centered portable hip exoskeleton: actuator, wearable interface, controller. *IEEE Trans. Med. Robot. Bionics*. 5:1–12, 2025.
39. Katz, B., J. Di Carlo, and S. Kim. Mini cheetah: a platform for pushing the limits of dynamic quadruped control. In: Proc. 2019 International Conference on Robotics and Automation (ICRA). IEEE, pp. 6295–6301.
40. Wensing, P. M., A. Wang, S. Seok, D. Otten, J. Lang, and S. Kim. Proprioceptive actuator design in the mit cheetah: impact mitigation and high-bandwidth physical interaction for dynamic legged robots. *IEEE Trans. Robot.* 33(3):509–522, 2017.
41. Farris, D. J., G. A. Lichtwark, N. A. Brown, and A. G. Cresswell. Deconstructing the power resistance relationship for squats: a joint-level analysis. *Scand. J. Med. Sci. Sports*. 26(7):774–781, 2016.
42. Armstrong, H. G. Anthropometry and mass distribution for human analogues. Military Male Aviators, 1, 1988.
43. Seth, A., M. Sherman, J. A. Reinbolt, and S. L. Delp. OpenSim: a musculoskeletal modeling and simulation framework for in silico investigations and exchange. *Procedia IUTAM*. 2:212–232, 2011.
44. Brockway, J. Derivation of formulae used to calculate energy expenditure in man. *Hum. Nutr. Clin. Nutr.* 41(6):463–471, 1987.
45. Jackson, A. S. Estimating maximum heart rate from age: is it a linear relationship? *Med. Sci. Sports Exerc.* 39(5):821–821, 2007.
46. Luo, S., G. Androwis, S. Adamovich, H. Su, E. Nunez, and X. Zhou. Reinforcement learning and control of a lower extremity exoskeleton for squat assistance. *Front. Robot. AI*. 8:702845, 2021.